PHYSICAL REVIEW C **68**, 011602(R) (2003)

Excitation and decay of projectilelike fragments formed in dissipative peripheral collisions at intermediate energies

R. Yanez, S. Hudan, R. Alfaro, B. Davin, Y. Larochelle, H. Xu, L. Beaulieu, T. Lefort, V. E. Viola, and R. T. de Souza
Department of Chemistry and Indiana University Cyclotron Facility, Indiana University, Bloomington, Indiana 47405, USA

T. X. Liu, X. D. Liu, W. G. Lynch, R. Shomin, W. P. Tan, M. B. Tsang, A. Vander Molen, A. Wagner, and H. F. Xi
National Superconducting Cyclotron Laboratory and Department of Physics and Astronomy, Michigan State University, East Lansing, Michigan 48824, USA

R. J. Charity and L. G. Sobotka
Department of Chemistry, Washington University, St. Louis, Missouri 63130, USA

(Received 3 April 2003; published 31 July 2003)

Projectilelike fragments (PLF, $15 \leqslant Z \leqslant 46$) formed in peripheral and midperipheral collisions of ^{114}Cd projectiles with ^{92}Mo nuclei at $E/A = 50$ MeV have been detected at very forward angles, $2.1° \leqslant \theta_{lab} \leqslant 4.2°$. Calorimetric analysis of the charged particles observed in coincidence with the PLF reveals that the excitation of the primary PLF is strongly related to its velocity damping. Furthermore, for a given V_{PLF*}, its excitation is not related to its size, Z_{PLF*}. For the largest velocity damping, the excitation energy attained is large, approximately commensurate with a system at the limiting temperature.

DOI: 10.1103/PhysRevC.68.011602 PACS number(s): 25.70.Mn

The nuclear equation of state (EOS), and in particular its isospin dependence, is a topic of fundamental interest [1]. For finite nuclei, examination of the limiting temperature, the maximum temperature attainable [2–4], provides information on the interplay between the nuclear EOS and Coulomb instabilities. To date, a variety of means have been used to excite finite nuclear matter to the limits of stability. These approaches range from multi-GeV hadronic probes [5,6] or projectile fragmentation at relativistic energies [7,8], to central collisions of intermediate-energy heavy ions [9–11]. Recent advances in the availability of high-intensity radioactive beams in the intermediate-energy domain raise the question of how the N/Z dependence of the EOS is best probed. While it is widely accepted that nuclear matter at high excitation can be formed by central collision of two heavy ions, this approach has several drawbacks in probing the N/Z dependence of the EOS. Interaction of a projectile with extreme N/Z with a stable target results in a system with N/Z less exotic than the projectile. Furthermore, the fragmenting source in a central collision is poorly defined in size, density, and N/Z. In contrast to central collisions, peripheral collisions result, with large cross section, in the survival of a projectilelike nucleus and a targetlike nucleus, both at near normal density. Previous studies have examined the decay of the excited projectilelike fragments produced in peripheral collisions [12–14].

In this Rapid Communication, we focus on the correlation between the excitation of the projectilelike fragment (PLF) resulting from peripheral and midperipheral collisions, and its associated velocity damping. When selected on velocity dissipation, we determine that the size of the PLF has essentially no impact on its total excitation. Moreover, our results indicate that midperipheral collisions of two intermediate-energy heavy ions can result in the formation of a projectilelike fragment excited to the limits of stability.

The experiment was conducted at Michigan State University where a beam of ^{114}Cd nuclei accelerated by the K1200 cyclotron to $E/A = 50$ MeV impinged on a ^{92}Mo foil 5.45 mg/cm^2 thick. At very forward angles ($2.1° \leqslant \theta_{lab} \leqslant 4.2°$) charged reaction products were detected by an annular ring Si/CsI(Tl) telescope (RD) [15]. For $Z \leqslant 48$, this telescope provided both good charge ($\delta Z/Z \sim 0.25$) and angular ($\Delta\theta = 0.125°; \Delta\phi = 22.5°$) resolution. Light charged particles ($Z \leqslant 2$) and intermediate mass fragments (IMFs, $3 \leqslant Z \leqslant 10$) emitted at larger angles ($7° \leqslant \theta_{lab} \leqslant 58°$) were isotopically identified in the large area silicon strip array, LASSA [16,17]. Charged-particle multiplicity was measured using the MSU Miniball [18] and Washington University Miniwall. A trigger condition of three charged particles in the Miniball/Miniwall was used during the experiment.

An overall qualitative description of the reaction is provided in Fig. 1. With increasing charged-particle multiplicity N_c, the most probable atomic number of the PLF, Z_{PLF}, detected in the RD decreases. While the relationship between these two quantities for $N_c \leqslant 15$ is approximately linear, for larger multiplicities Z_{PLF} depends more weakly on N_c. Moreover, while the correlation between the most probable values is clearly evident, it is noteworthy that the distribution is broad in both Z_{PLF} and N_c. The relationship between the size of the PLF, as represented by Z_{PLF}, and the velocity of the PLF, V_{PLF}, is shown in Fig. 1(b). As the atomic number of the PLF decreases from $Z = 48$, one observes a gradual decrease from the projectile velocity, indicated by the arrow i.e., consistent with velocity damping of the PLF. For $Z \leqslant 38$ the most probable velocity is relatively constant with a value of approximately 9.0 cm/ns, corresponding to 95% of V_{beam}. In contrast to this constancy, the minimum velocity attained decreases (maximum damping increases) with decreasing Z_{PLF}. While these observations are consistent with previous experimental measurements, in this work we focus on the characteristics of the PLF: specifically, its size (Z_{PLF}) and velocity damping.

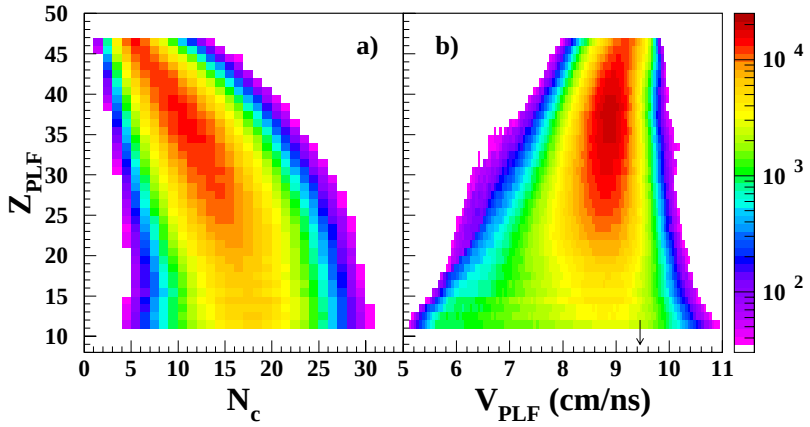

FIG. 1. (Color online) (a) Relationship between the measured charged-particle multiplicity N_c and the atomic number of the detected PLF, Z_{PLF}. (b) Correlation between Z_{PLF} and its velocity in the laboratory, V_{PLF}. The arrow indicates the beam velocity.

To examine the excitation of the PLF formed in peripheral collisions, we required the detection of a single fragment in the RD with $15 \leqslant Z \leqslant 46$ and a velocity larger than the center-of-mass velocity. The magnitude of the most probable velocity of this fragment (95% of V_{beam}) suggests that it is a remnant of the projectile following the interaction stage of the collision and deexcitation. For clarity, we subsequently refer to the primary excited projectilelike fragment as the PLF* and the detected nucleus following deexcitation as the PLF. The characteristics of the PLF*, namely, its Z, A, and velocity can be reconstructed by measuring the PLF residue and examining the multiplicities, kinetic-energy spectra, and angular distribution of coincident particles.

The energy-angle correlation for α particles detected in LASSA in the reference frame of the PLF* is displayed in Fig. 2(a). All quantities have been corrected for the geometric efficiency of LASSA, as well as recoil due to emission. A prominent feature evident is the horizontal ridge observed for $\theta_{PLF*} > 40°$. This ridge can be understood as statistical emission of α particles from the PLF*. Emission at small angles $\theta_{PLF*} < 30°$ and large angles $\theta_{PLF*} > 160°$ is not observed due to the finite experimental acceptance. At backward angles, $\theta_{PLF*} > 120°$, one observes a second component in the two-dimensional spectrum. This component, which exhibits higher average energies, is a general feature of noncentral intermediate-energy heavy-ion collisions and has been associated with dynamical processes [19–21]. It is evident from Fig. 2(a) that for $\theta_{PLF*} < 90°$ the statistical emission process dominates, suggesting minimal dynamical contamination in this region.

In Fig. 2(b), the α particle kinetic-energy spectra are shown for six discrete angles $45° \leqslant \theta_{PLF*} \leqslant 70°$ with $\Delta\theta_{PLF*} = 1°$. To facilitate the comparison of the different spectra, the solid line depicts a single fit, performed for $\theta_{PLF*} = 55°$, to a Maxwell-Boltzmann distribution (as described below). Enhanced yield in the kinetic-energy spectra for $E \geqslant 40$ MeV can be understood as prompt α emission prior to attainment of equilibrium by the PLF*. As the exponential slopes of the kinetic-energy spectra reflect the excitation of the emitting source [22], the overlap of the different spectra with the single exponential in Fig. 2(b) indicates that in this angular range, both the α yield and emission temperature are relatively constant, consistent with decay of a single isotropically emitting source.

The correlation between the excitation of the PLF*, evidenced by the kinetic character of emitted particles, and its velocity damping is examined in Fig. 3. In this figure, the kinetic-energy distributions of p and α, emitted in the range $40° < \theta_{PLF*} < 75°$, are shown selected on decreasing velocity of the PLF*, V_{PLF*}. One qualitatively observes that all the distributions are approximately Maxwellian in shape with a notable flattening of the exponential slope with decreasing V_{PLF*}, i.e., increased velocity damping. For the uppermost spectra, which correspond to the lowest velocity damping,

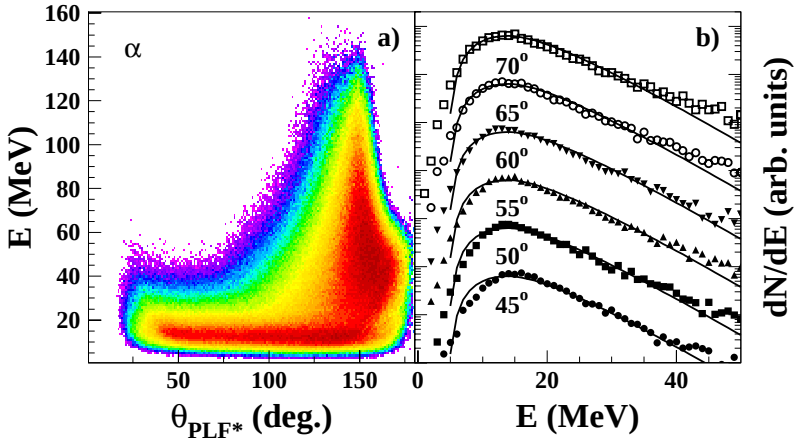

FIG. 2. (Color online) (a) Energy-angle correlation for α particles, in the PLF* frame. Color represents the relative probability on a logarithmic scale. (b) Kinetic-energy spectra for α particles in the PLF* frame for the indicated angles with a vertical displacement of a factor of 10 for clarity.

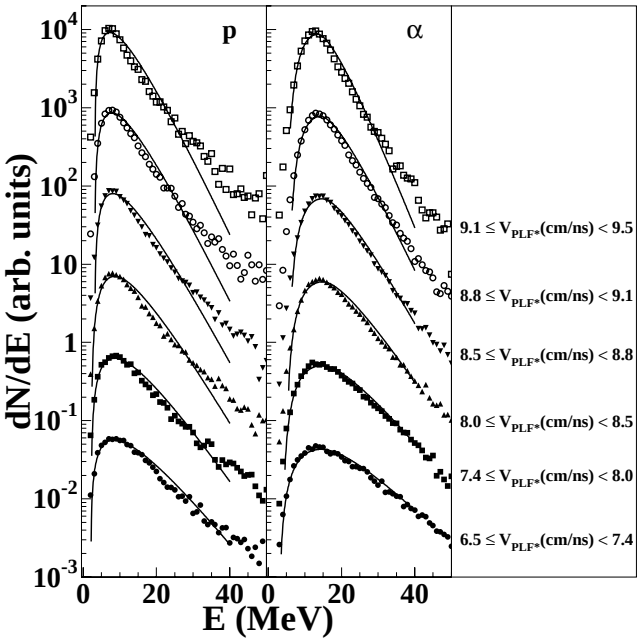

FIG. 3. Kinetic-energy spectra for p and α particles emitted forward of the PLF* associated with different velocity, V_{PLF*}. Velocity selections are shown in the right-hand panel. Spectra have been displaced vertically by a factor of 10 for clarity. Solid lines depict the result of fitting the spectra with a Maxwell-Boltzmann distribution. See text for details.

deviation from the single exponential behavior is evident. This deviation from the single exponential behavior, which does not contribute significantly to the total yield of detected particles, can be attributed to preequilibrium emission. At low velocity damping, i.e., low excitation, suppression of the statistical component maximizes the separation of the preequilibrium and equilibrium components. Comparison of the measured yield with the single source fit suggests that these preequilibrium processes constitute $\approx 2\%$ of the total PLF* yield. To quantify the dependence of the exponential spectral tail on V_{PLF*} for isotopically identified particles, we have fit the spectra selected on V_{PLF*}.

The fitting function used was [23]

$$N(\epsilon) = 0 \quad \text{if} \quad \epsilon \leqslant B', \tag{1}$$

$$N(\epsilon) \propto C'(\epsilon - B')^D \exp\left(-\frac{\epsilon}{T_s}\right) \quad \text{if} \quad B' < \epsilon < B + T_s, \tag{2}$$

$$N(\epsilon) \propto (\epsilon - B)\exp\left(-\frac{\epsilon}{T_s}\right) \quad \text{if} \quad \epsilon \geqslant B + T_s, \tag{3}$$

where $C' = T_s/(DT_s)^D$ and $B' = (1-D)T_s + B$. The parameter ϵ represents the kinetic energy, while B is a barrier parameter and D a barrier diffuseness and penetrability parameter. The parameter T_s, which characterizes the exponential, can be related within a statistical framework to the energy dependence of the density of states in the daughter nucleus following decay. The extracted slope parameter T_s reflects the average excitation of the distribution of nuclei decaying

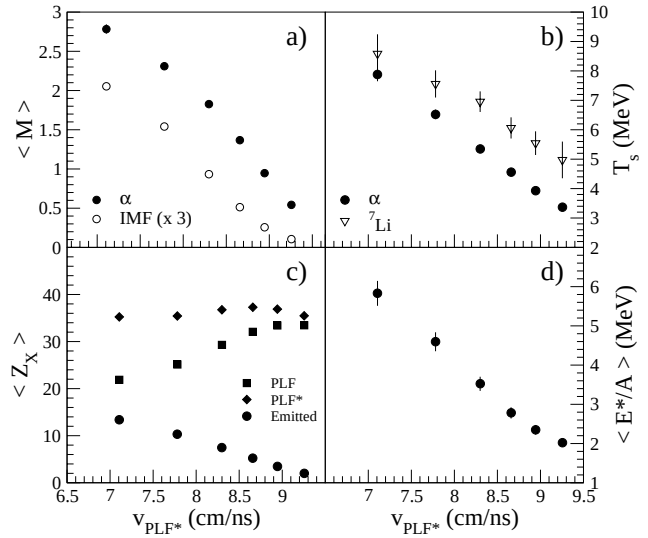

FIG. 4. (a) Extracted average multiplicities for α particles and IMFs as a function of V_{PLF*}. (b) Relation between the extracted slope parameters for α particles and ^{7}Li fragments emitted from the PLF* and V_{PLF*}. (c) Dependence of $\langle Z_{emitted}\rangle$, $\langle Z_{PLF}\rangle$, and $\langle Z_{PLF*}\rangle$ on V_{PLF*}. (d) Excitation energy scale deduced by calorimetry for different velocity dissipation.

via the specific particle decay selected. The resulting fits are shown as solid lines in Figs. 2 and 3. A qualitative feature readily apparent in Fig. 3 is that the p and α spectra exhibit exponential tails of similar magnitude for a given V_{PLF*}. Although similar in magnitude, the extracted slope parameters are not identical. While at the lowest excitation the slope parameters are approximately equal, at high excitation the proton slope parameters are lower than the α slope parameters by 1.2–1.3 MeV, probably due to differences in the deexcitation cascade.

To extract the multiplicities of particles emitted from the PLF*, we assume isotropic emission from the PLF*, consistent with the emission pattern shown in Fig. 2. This assumption is supported by the angular distribution of particles forward of the PLF*. For example, for α particles with $E \leqslant 25$ MeV in the PLF* frame, the yield is essentially constant, increasing by $\approx 15\%$ as θ_{PLF*} increases from 50° to 90°. By assuming all particles emitted forward of the PLF* ($V_\parallel > V_{PLF*}$) can be attributed to the PLF* and accounting for the geometric acceptance, we deduced the total multiplicity of charged particles evaporated from the PLF*. The dependence of the average extracted multiplicities $\langle M\rangle$ and slope parameters T_s on V_{PLF*} is displayed in Figs. 4(a) and 4(b). With decreasing V_{PLF*}, the average multiplicity of emitted α particles, indicated by the filled symbols in Fig. 4(a), increases from 0.5 to 2.75, a factor of approximately 5. The multiplicity of IMFs ($3 \leqslant Z \leqslant 8$) exhibits an increase from ≈ 0.03 to ≈ 0.7 over the same interval. Along with the increase in the charged-particle multiplicity, the slope parameter T_s for α particles increases from 3.4 to 8.0, i.e., by a factor of approximately 2, as shown by the filled circles in Fig. 4(b). The dependence of T_s on V_{PLF*} for ^{7}Li fragments—representative of IMFs—is also shown in Fig. 4(b) by the open symbols. The monotonic increase with ve-

locity damping observed for α particles is also manifested for ^{7}Li fragments. In comparison to the α slopes, the T_s values for ^{7}Li fragments are larger in magnitude, most likely reflecting an earlier emission time as compared to α particles. The monotonic increase in both T_s and $\langle M \rangle$ with decreasing V_{PLF*} can be understood as the increased excitation of the PLF* with increasing velocity dissipation. From the measured multiplicities of emitted particles, we have calculated the average emitted charge, from the PLF* $\langle Z_{emitted} \rangle = \Sigma \langle M_i \rangle Z_i$. With increasing velocity dissipation, $\langle Z_{emitted} \rangle$ increases from ≈ 2 to ≈ 14 as shown in Fig. 4(c) by the open symbols. Coupled with this increase is a concurrent decrease of the detected $\langle Z_{PLF} \rangle$ from ≈ 34 to ≈ 22, indicated by the filled squares. As can be seen from the solid diamonds in Fig. 4(c), $\langle Z_{PLF*} \rangle = \langle Z_{PLF} \rangle + \langle Z_{emitted} \rangle$ has a near constant value of ≈ 36–38, ≈ 75–$80\,\%$ of $Z_{projectile}$, for all values of V_{PLF*}. The reason $\langle Z_{PLF*} \rangle$ does not equal $Z_{projectile}$ even for the lowest velocity dissipation is due to the experimental hardware trigger of $N_c \geqslant 3$ in the Miniball/Miniwall, which suppresses the most peripheral collisions. The impact of charged-particle multiplicity selection in suppressing the most peripheral collisions has been established previously [24,25].

In order to determine the excitation of the PLF* we have performed a calorimetric analysis [26,27]. Using the extracted average multiplicity and the measured average kinetic energy for each type of particle evaporated from the PLF*, we deduce the average excitation energy of the PLF* following preequilibrium emission. As the mass of the PLF was not measured, we assumed its mass based upon the EPAX systematics [28]. The average mass of the PLF* was assumed to be given by $\langle A_{PLF*} \rangle = (A/Z)_{projectile} \langle Z_{PLF*} \rangle$. The average neutron multiplicity was deduced by mass conservation and their average energy of was taken as $\langle E^n \rangle = \langle E^p \rangle - (0.106 * Z_{PLF*} - 0.9)$ [29]. In order to calculate the $\langle Q \rangle$ we assumed $\langle Q \rangle = \Delta m(A_{PLF*}, Z_{PLF*}) - [\Delta m(A_{PLF}, Z_{PLF}) + \langle Q_{emitted} \rangle$ where $\langle Q_{emitted} \rangle = \Sigma \langle M_i \rangle \Delta m_i$ with i ranging over all charged particles and neutrons emitted, where Δm is the mass defect. Within this framework, we deduce the relation between V_{PLF*} and E^*/A shown in Fig. 4(d).

The deduced relationship between E^*/A and velocity damping exhibits an essentially linear behavior over the entire range of velocity dissipation. This relationship is significant as it has been generally accepted that the excitation of the PLF* depends on the overlap between projectile and target [13] and *not* on velocity dissipation. Furthermore, we observe that for the most damped collisions, which correspond to $\approx 75\%$ of V_{beam}, i.e., considerable velocity damping, an excitation of approximately 6 MeV/nucleon is attained.

It is important to place the maximum excitation observed for these midperipheral collisions in context. The excitation energy observed is comparable to the excitation for which one observes the onset of a plateau in the caloric curve for an $A = 90$ nucleus [4]. Moreover, the selection of the survival of a large residue (the PLF) favors lower excitation. From this analysis it is clear that an excitation comparable to that observed for a central collision of two intermediate-energy heavy ions has been attained for midperipheral heavy-ion collisions at $E/A = 50$ MeV.

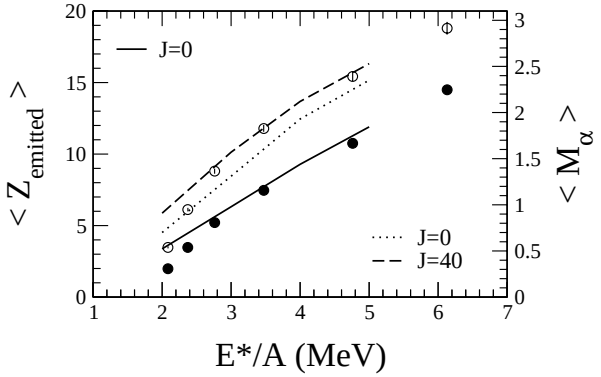

FIG. 5. Dependence of $\langle Z_{emitted} \rangle$ and $\langle M_\alpha \rangle$ on E^*/A. Solid symbols and line refer to $\langle Z_{emitted} \rangle$ while open symbols and broken lines refer to $\langle M_\alpha \rangle$. For the experimental data (symbols) the excitation scale is deduced by calorimetry, while for the GEMINI calculations (lines) it corresponds to the initial excitation of the emitting source. In GEMINI, $\langle Z_{emitted} \rangle$ for the $J = 0$ and $40\,\hbar$ calculations overlap each other.

To assess the sensitivity of the deduced E^*/A within the calorimetric approach to the spin of the emitting PLF*, we

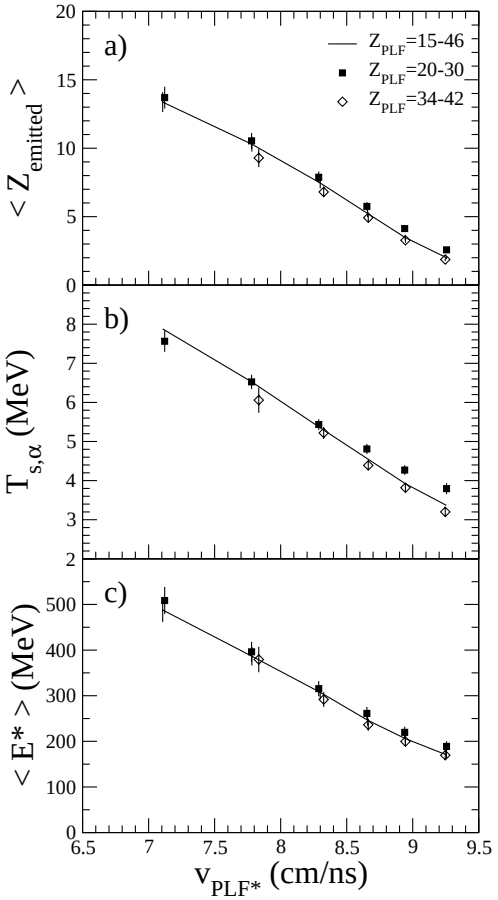

FIG. 6. Dependence of $\langle Z_{emitted} \rangle$, $T_{s,\alpha}$, and $\langle E^* \rangle$ on V_{PLF*} selected on Z_{PLF}.

utilized the statistical model code GEMINI [30]. The code GEMINI employs a Hauser-Feshbach formalism to describe the statistical emission of particles from a nucleus of (Z,A) characterized by an excitation energy E^* and a spin J. We varied the excitation of the source between 2 MeV/nucleon and 5 MeV/nucleon with an initial $Z=38$ (deduced from the data) and $A=90$. We explored the sensitivity of the deduced E^*/A to spin by calculations at $J=0$ and $40\hbar$. The results of these calculations are depicted by the different lines in Fig. 5. The calculated $\langle Z_{emitted}\rangle$ is quite insensitive to the assumed spin of the decaying nucleus for a constant total E^* while $\langle M_\alpha\rangle$ manifests a modest sensitivity. From the GEMINI calculations we conclude that $\langle Z_{emitted}\rangle$ is fairly insensitive to the spin of the decaying nucleus, supporting the excitation scale deduced for the data.

We have examined whether the correlation between excitation and velocity damping observed in Fig. 4(d) depends on the size of the observed PLF, Z_{PLF}. The dependence of $Z_{emitted}$, T_s, and deduced $\langle E^*\rangle$ on V_{PLF*} is displayed in Fig. 6 selected on Z_{PLF}. Quite strikingly, one finds that the monotonic increase of $Z_{emitted}$ and T_s with decreasing V_{PLF*}, previously observed, is independent of Z_{PLF}. Moreover, different Z_{PLF} with the same velocity damping manifest the same average total excitation $\langle E^*\rangle$, resulting in different $\langle E^*/A\rangle$. We have associated Z_{PLF*} with b/b_{max} in a geometrical model of two overlapping nuclei. From this geometrical model and the results in Fig. 6, one concludes that for $0.4\leqslant b/b_{max}\leqslant 1.0$, velocity dissipation determines the excitation of the PLF*. For the impact parameter range examined, the most probable velocity dissipation is low, and does not change significantly with decreasing Z_{PLF} [Fig. 1(b)], suggesting that the most probable excitation of the projectile (and target) spectator is moderate ($\approx$200 MeV) and approximately constant with impact parameter. Systems formed at high excitation represent a small fraction of the cross section.

We have carefully examined all possible sources of bias in our measurement and analysis and find no systematic bias that is responsible for the observed results. We therefore turn to understanding the observed correlations. One possibility in explaining these results is that for each impact parameter a distribution of contact times exists. While the impact parameter determines the size of the PLF*, it is the contact time that determines the velocity dissipation and the excitation of the PLF*. Reaction models in the intermediate-energy domain need to account for the underlying mechanism responsible for the distribution of velocity damping (contact time), as well as the fundamental association between velocity damping and the PLF* excitation.

In summary, for peripheral collisions of a near symmetric system at $E/A=50$ MeV, highly excited projectilelike fragments are formed and *the excitation of the PLF* is associated with its velocity dissipation*. Moreover, when selected on velocity dissipation, *the total excitation of the PLF* does not depend on its size*. Selection of PLF of different size, but the same velocity dissipation, corresponds to the same excitation energy. Remarkably, *for the largest velocity dissipation an excitation energy approximately consistent with the limiting temperature is deduced*, presenting interesting opportunities for probing the N/Z dependence of the limiting temperature.

We would like to acknowledge the valuable assistance of the staff at MSU-NSCL for providing the high-quality beams that made this experiment possible. This work was supported by the U.S. Department of Energy under Contract Nos. DE-FG02-92ER40714 (IU), DE-FG02-87ER-40316 (WU) and the National Science Foundation under Grant No. PHY-95-28844 (MSU).

[1] B.A. Li, Phys. Rev. Lett. **88**, 192701 (2002).
[2] P. Bonche, Nucl. Phys. **A436**, 265 (1985).
[3] J. Natowitz *et al.*, Phys. Rev. Lett. **89**, 212701 (2002).
[4] J. Natowitz *et al.*, Phys. Rev. C **65**, 034618 (2002).
[5] T. Lefort *et al.*, Phys. Rev. C **64**, 064603 (2001).
[6] L. Beaulieu *et al.*, Phys. Rev. C **64**, 064604 (2001).
[7] R.P. Scharenberg *et al.*, Phys. Rev. C **64**, 054602 (2001).
[8] C.A. Ogilvie *et al.*, Phys. Rev. Lett. **67**, 1214 (1991).
[9] E. Piasecki *et al.*, Phys. Rev. Lett. **66**, 1291 (1991).
[10] D.R. Bowman *et al.*, Phys. Rev. Lett. **67**, 1527 (1991).
[11] N. Marie *et al.*, Phys. Lett. B **391**, 15 (1997).
[12] B. Lott *et al.*, Phys. Rev. Lett. **68**, 3141 (1992).
[13] J. Peter, Nucl. Phys. **A593**, 95 (1995).
[14] D. Doré *et al.*, Phys. Lett. B **491**, 15 (2000).
[15] B. P. Davin, Ph.D thesis, Indiana University, 2001.
[16] B. Davin *et al.*, Nucl. Instrum. Methods Phys. Res. A **473**, 302 (2001).
[17] A. Wagner *et al.*, Nucl. Instrum. Methods Phys. Res. A **456**, 290 (2001).
[18] R.T. de Souza *et al.*, Nucl. Instrum. Methods Phys. Res. A **295**, 109 (1990).
[19] J. Toke *et al.*, Phys. Rev. Lett. **75**, 2920 (1995).
[20] F. Bocage *et al.*, Nucl. Phys. **A676**, 391 (2000).
[21] B. Davin *et al.*, Phys. Rev. C **65**, 064614 (2002).
[22] W. Benenson *et al.*, Annu. Rev. Nucl. Part. Sci. **99**, 27 (1994).
[23] J.P. Lestone *et al.*, Nucl. Phys. **A559**, 277 (1993).
[24] S. Baldwin *et al.*, Phys. Rev. Lett. **74**, 1299 (1995).
[25] G. Kunde *et al.*, Phys. Rev. Lett. **77**, 2897 (1996).
[26] J.C. Steckmeyer *et al.*, Nucl. Phys. **A500**, 372 (1989).
[27] D. Cussol, Nucl. Phys. **A561**, 298 (1993).
[28] K. Summerer, Phys. Rev. C **61**, 034607 (2000).
[29] W.E. Parker, Phys. Rev. C **44**, 774 (1991).
[30] R. Charity *et al.*, Phys. Rev. C **63**, 024611 (2001).